Paper II

II

Extraction of frequency-dependent reflection, transmission, and scattering parameters for short metal reflectors from FEM-BEM simulations

S. Härmä and V. P. Plessky

S. Härmä and V. P. Plessky, "Extraction of frequency-dependent reflection, transmission, and scattering parameters for short metal reflectors from FEM-BEM simulations", IEEE Transactions on Ultrasonics, Ferroelectrics, and Frequency Control, Vol. 55, No. 4, April 2008, pp. 883-889.

Extraction of Frequency-Dependent Reflection, Transmission, and Scattering Parameters for Short Metal Reflectors from FEM-BEM Simulations

Sanna Härmä and Victor P. Plessky, *Senior Member, IEEE*

***Abstract*—Reflectors comprised of only a single or a few electrodes provide controllable, weak reflectivity essential for surface acoustic wave (SAW) radio-frequency identification (RFID) tags. The reflection, transmission, and scattering parameters of such reflectors must be known as a function of frequency in order to be able to control the amplitudes of tag responses and to use phase-based encoding reliably.**

In this work, we present a method of extracting the main reflection, transmission, and scattering parameters for short metal reflectors as a function of frequency. We use test device *S* parameters obtained through finite- and boundary-element method (FEM-BEM)-based simulations and, as an example, determine the reflection and transmission coefficients (their absolute values and phase angles) and the energy scattered into bulk for a few different single-electrode reflectors. We compare these parameter values to earlier results.

Although only used for simulated data in this work, the same method can be applied to measured data as well. Assuming the *S* parameters available, this method is very fast and does not require any heavy calculation or special software.

I. Introduction

To achieve a reasonably high data capacity, a surface acoustic wave (SAW) radio-frequency identification (RFID) tag must include about 20 to 50 reflecting electrodes, which also implies that the reflectors, especially in the beginning of the code reflector array, must have very weak reflectivities and, thus, consist of only one or a few electrodes [1]–[3]. It is evident that the knowledge of reflection, transmission, and scattering parameters is essential in tag design. Moreover, in order to be able to control the amplitudes of tag response signals and to use phase-based encoding reliably, the parameters related to reflection and transmission must be known as a function of frequency.

Previously, Lehtonen *et al.* [3]–[5] have done a series of work to determine the reflection and scattering parameters of reflectors consisting of one to three electrodes as a function of relative metal thickness (h/λ) and metallization ratio (a/p). They have used test device Y parameters produced by a finite- and boundary-element method (FEM-BEM)-based simulation software, obtained the impulse response through Fourier transformation, and used time-gating to separate the reflective echoes. However, their results do not give the parameter values as a function of frequency. The frequency dependence of reflection, transmission, and scattering parameters has been studied recently by Wang *et al.* [6]. They have developed a source regeneration method based on Green's function theory and FEM-BEM that directly calculates the reflection, transmission and scattering parameters at each frequency point of a specified range of frequencies. Determining the parameters is faster this way, but it includes evaluation of the energy of scattered waves, which is difficult to accomplish experimentally.

In this work, we present an alternative method for determining the reflection, transmission, and scattering parameters of short metal reflectors as a function of frequency. We use the FEM-BEM-computed S parameter data of a primitive SAW tag test device as a starting point. FEM-BEM is nowadays often used for characterization of waves in complicated structures [7]. We determine the reflection and transmission coefficients (absolute values and phase angles) and the energy scattered into bulk in a simple and very fast way without any heavy calculation or special software (assuming the S parameters are available). Our analysis also yields the free-surface attenuation parameter and the free-surface SAW velocity. The method developed in this work can be applied to measured data without any significant changes.

II. Method

Our method involves analyzing the response of a simple SAW tag test device consisting of an interdigital transducer (IDT) and three single-electrode reflectors. The device is simulated using FEMSAW [8], a FEM-BEM-based [9] simulation software which produces the Y (or S) parameters of a studied structure for a range of frequencies. We develop an analytical method to extract the reflection and transmission coefficients (absolute values and phase angles) and the energy scattered into bulk as a function of frequency by using the output of FEMSAW. In addi-

Manuscript received September 12, 2007; accepted January 3, 2008.

The authors are with the Department of Engineering Physics, Helsinki University of Technology, FI-02015 TKK, Finland (e-mail: sanna.harma@tkk.fi).

V. P. Plessky is also with GVR Trade SA, Bevaix, Switzerland.

Digital Object Identifier 10.1109/TUFFC.2008.724

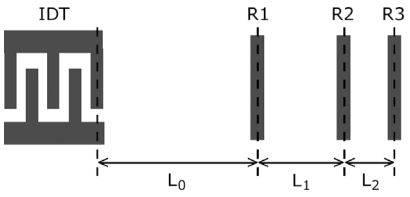

Fig. 1. Test structure geometry. $L_0 = 3000.000\ \mu$m, $L_1 = 600.000\ \mu$m, and $L_2 = 362.618\ \mu$m (the reference planes are located at the centers of the reflectors and at the center of the right-most IDT electrode).

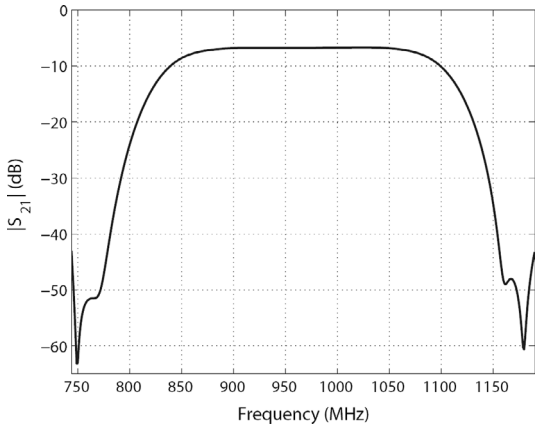

Fig. 2. $|S_{21}|$ for a delay line consisting of two identical IDTs facing each other and separated by 100 μm.

tion, this method also yields the free-surface attenuation parameter and the free-surface SAW velocity.

A. Test Structures

The geometry of the studied structure is shown schematically in Fig. 1. The IDT used for generation and reception of SAW is of standard type and has 10 electrodes with alternating polarities. Its electrode pitch is 2 μm, metallization ratio 0.5, and aperture 100 μm. The substrate material is 128°-$LiNbO_3$. The absolute value of the simulated S_{21} parameter of a delay line consisting of two such IDTs facing each other and separated by 100 μm is shown in Fig. 2. The center frequency lies at about 970 MHz.

The three identical reflectors placed in the acoustic path each consist of a single floating electrode. The distances $L_0 = 3000.000\ \mu$m, $L_1 = 600.000\ \mu$m, and $L_2 = 362.618\ \mu$m (shown in Fig. 1) between the reflectors have been chosen such that none of the first four reflections overlap with any other reflection. Three of these signals are direct reflections from the three single-electrode reflectors described above, and the fourth signal is a result of multiple reflections from these reflectors. L_0 is measured from the center of the right-most electrode of the IDT to the center of the first reflector. L_1 and L_2 are defined as the center-to-center distances of the first and second reflector (R1 and R2) and the second and third reflector (R2 and R3), respectively.

FEMSAW simulations were carried out for three test structures: TS1, TS2, and TS3. Each of these devices has the geometry depicted in Fig. 1. However, metal thickness and reflector width are different in each device. These parameters are summarized in Table I. In order to facilitate comparisons with the results of Lehtonen *et al.* [3]–[5] and Wang *et al.* [6], we have adopted here the concept of electrode pitch, although it is not normally a relevant parameter for single-electrode reflectors. We take the pitch p as 2 μm, which roughly corresponds to half the wavelength λ around 1000 MHz. In accordance, the relative metal thickness h/λ is evaluated as $h/(2p)$. For each test device, the IDT has the same metal thickness as the single-electrode reflectors. It is also to be noted that, apart from the varying metal thickness, IDTs have the same geometry in each test device.

TABLE I
METAL THICKNESSES AND REFLECTOR WIDTHS FOR SIMULATED STRUCTURES.

Test structure	Metal thickness h (Å)	Relative metal thickness h/λ (%)	Reflector width a (μm)	Metal ratio a/p
TS1	1000	2.5	0.8	0.4
TS2	2000	5.0	1.2	0.6
TS3	400	1.0	1.0	0.5

B. Simulations

The analysis presented in this work is based on the S_{11} parameter obtained through FEMSAW simulations. The simulations were run for the frequency range of 740 MHz to 1200 MHz with a frequency step of 0.1 MHz. This yields, after an inverse Fourier transformation, a time frame of 10 μs and a time step of 2.2 ns. The resistive losses in the metal electrodes and the propagation loss on 128°-$LiNbO_3$ were not taken into account in order to be able to compare the results with those of Lehtonen and Wang.

The simulation was first carried out separately for the entire SAW tag structure described above and for a structure consisting of the IDT only. The absolute value of the S_{11} parameter for these two cases is shown in Fig. 3. The S_{11} parameter of the IDT then was subtracted from the S_{11} parameter of the entire device. The subtraction was performed in linear scale for the real and imaginary parts of S_{11}. In this way, the data to be analyzed contains only the response of the reflectors and is clear of any contribution from the direct signal reflections from the IDT (due to electrical mismatch). The absolute value of the result of subtraction is shown in Fig. 4.

To obtain the time response, the result of subtraction is Fourier transformed into the time domain. However, the data must be weighted before transformation. In order to avoid any unwanted components that might arise from a Fourier transformation of a function defined only at a limited frequency range and having different values at the ends of this range, a weight function must be applied, which takes the function values to very small (or equal)

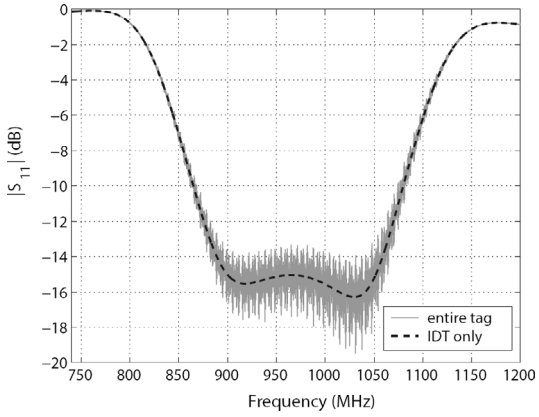

Fig. 3. $|S_{11}|$ for entire tag (solid line) and $|S_{11}|$ for IDT alone (dashed line).

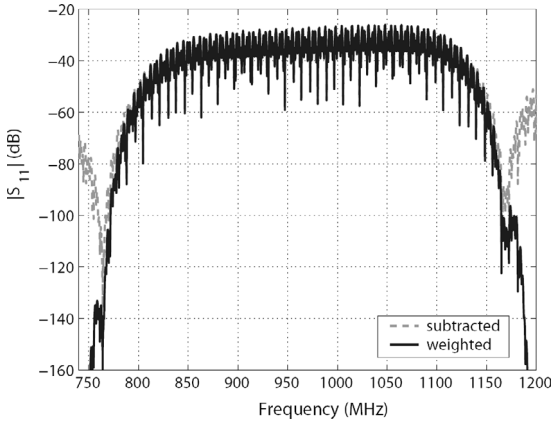

Fig. 4. Absolute value of the difference of S_{11} for the entire tag and S_{11} for the IDT alone (dashed: without weighting, solid: with weighting).

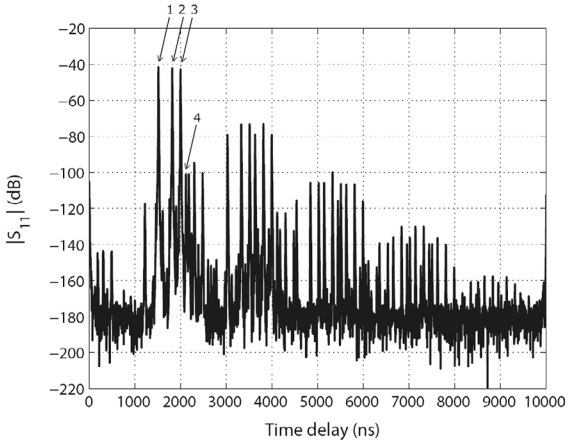

Fig. 5. $|S_{11}|$ of the 3-reflector SAW tag in time domain. First four reflections are indicated by numbers 1 through 4.

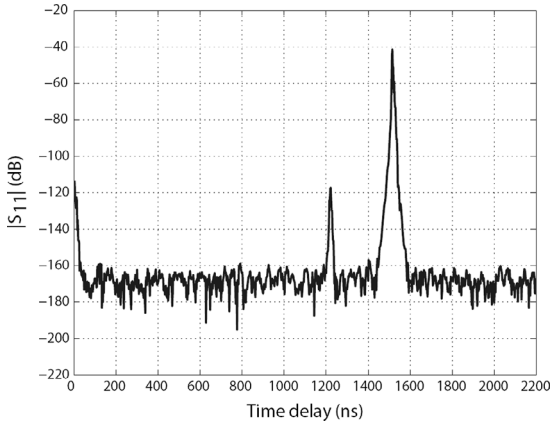

Fig. 6. $|S_{11}|$ of the 1-reflector SAW tag in time domain.

values at the ends of the studied frequency range. The weighted curve is shown in Fig. 4.

Fig. 5 presents the obtained time response. As the time scale is quite long, many groups of multiple-transit signals are visible. However, we are primarily interested only in the first four reflections, that is, the reflections having the paths and time delays as summarized in Table II. As mentioned above, the first three signals are direct reflections from reflectors R1, R2, and R3 (SAWs are generated and received by the same IDT). The fourth signal is a result of multiple reflections from R1 and R2. For the analysis, we need the frequency-dependent S_{11} parameter for each of these four reflections separately. These signals are obtained by time-gating the response shown in Fig. 5. In order to see which signals originate from which reflections and for an accurate determination of the beginning and end of each reflection, a FEMSAW simulation was run for two additional structures: 1) IDT and R1 and 2) IDT, R1, and R2. The resulting $|S_{11}|$ for these simulations are shown in Figs. 6 and 7. Fig. 8 shows the three-reflector case with time-gating imposed on the four reflections of interest. Fig. 9 presents the time-gated signals after Fourier transformation back to the frequency domain. The weighting function has been removed from the signals shown in Fig. 9. The first three echoes are of practically equal amplitude, which is evident as they correspond to identical reflectors and because propagation loss is assumed negligible. The fourth echo has undergone three reflections and is naturally of lower amplitude. Fig. 10 shows the first three reflections on a scale different from that in Fig. 9.

TABLE II
PATHS AND DELAYS OF THE FIRST FOUR REFLECTIONS.

Signal	Path	Delay (ns)
1st	IDT - R1 - IDT	1514
2nd	IDT - R2 - IDT	1817
3rd	IDT - R3 - IDT	1999
4th	IDT - R2 - R1 - R2 - IDT	2118

C. Analysis of S_{11} Parameter

Denoting the i^{th} reflected signal (the time-gated S_{11} parameter related to the i^{th} reflection) by S_i, we can write each of the four signals of interest as a product of a

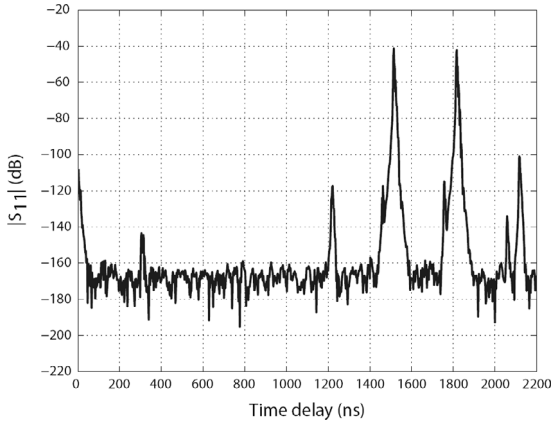

Fig. 7. $|S_{11}|$ of the two-reflector SAW tag in time domain.

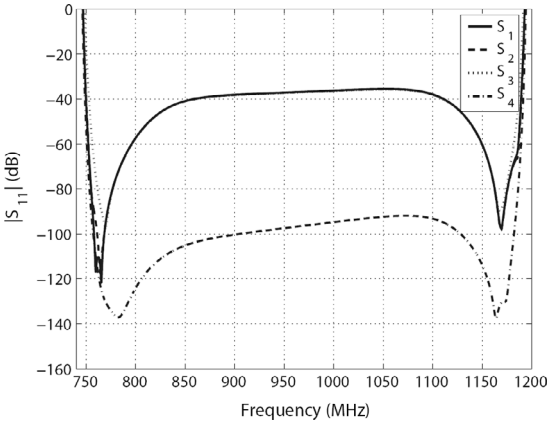

Fig. 9. First four reflections in frequency domain.

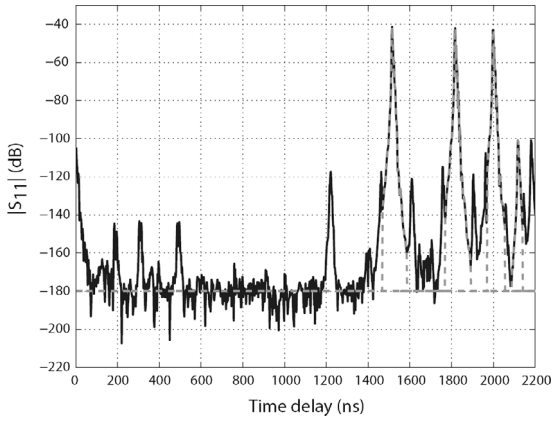

Fig. 8. $|S_{11}|$ of the three-reflector SAW tag in time domain and time-gating of reflections.

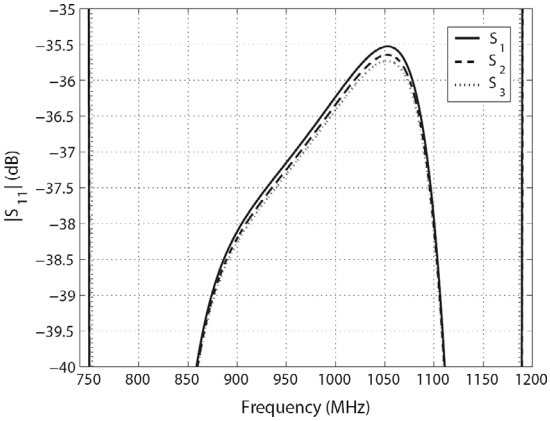

Fig. 10. First three reflections in frequency domain. Scale different from that in Fig. 9.

frequency-dependent factor F_i and the original signal S_0 used for exciting the device as follows:

$$S_i = F_i S_0 \quad (i = 1, \ldots, 4), \tag{1}$$

where:

$$F_1 = DP_0RP_0D = D^2P_0^2R, \tag{2}$$
$$F_2 = D^2P_0^2T^2P_1^2R, \tag{3}$$
$$F_3 = D^2P_0^2T^4P_1^2P_2^2R, \tag{4}$$
$$F_4 = D^2P_0^2T^2P_1^4R^3. \tag{5}$$

In (2) to (5), D is the transduction coefficient of the IDT. P_0, P_1, and P_2 are the coefficients related to propagation on free surface and have the form $P_i = e^{-\alpha L_i - jkL_i}$, where α is the free-surface attenuation coefficient, k is the wavenumber, and L_i refers to the distances between the elements of the device (the reference planes are located at the centers of the reflectors and at the center of the right-most IDT electrode, see Fig. 1). The reflection and transmission coefficients are denoted by R and T, respectively, and have the forms $R = re^{j\varphi_R}$ and $T = te^{j\varphi_T}$, where the absolute values r and t also include the effect of losses within the metal reflectors. φ_R and φ_T are the phase shifts due to reflection and transmission, respectively. These phase shifts include the change of phase due to the difference in SAW velocities on free and metallized surfaces and the change of phase due to losses (if any), such as scattering into bulk. As D, α, k, r, t, φ_R, and φ_T are all frequency-dependent variables, also all variables in (2) to (5) are frequency dependent and thus described by arrays having the same number of elements as S_{11}. The products in (1) to (5) are calculated pointwise at each frequency. The same applies to (6) through (15) below.

The content of (1) can be written as:

$$\frac{S_2}{S_1} = T^2P_1^2, \tag{6}$$
$$\frac{S_3}{S_1} = T^4P_1^2P_2^2, \tag{7}$$
$$\frac{S_4}{S_2} = R^2P_1^2. \tag{8}$$

This system of equations can be solved for α and k by dividing the square of (6) by (7):

$$\frac{S_2^2}{S_1S_3} = \left(\frac{P_1}{P_2}\right)^2 = e^{-2\alpha(L_1-L_2)-2jk(L_1-L_2)}. \tag{9}$$

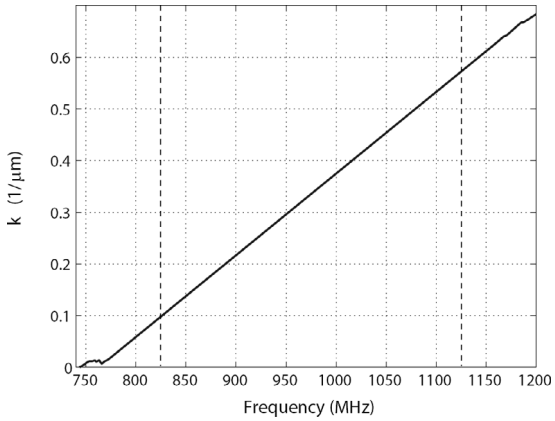

Fig. 11. Wavenumber k versus frequency. Reliable region between dashed lines.

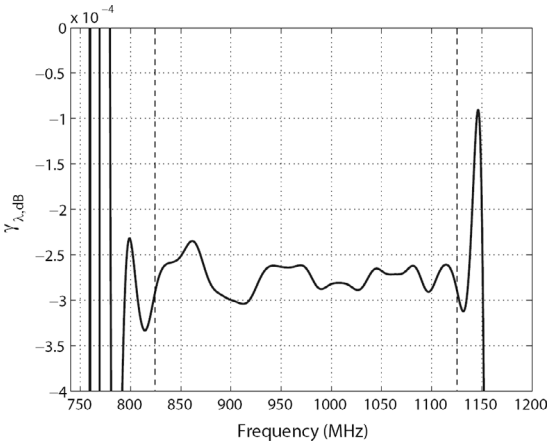

Fig. 12. Propagation loss parameter $\gamma_{\lambda,\mathrm{dB}}$ versus frequency. Reliable region between dashed lines.

Equating the absolute values and phase angles in (9) gives

$$\alpha = -\frac{1}{2(L_1 - L_2)} \ln \left| \frac{S_2^2}{S_1 S_3} \right|, \tag{10}$$

$$k = -\frac{1}{2(L_1 - L_2)} \angle \left(\frac{S_2^2}{S_1 S_3} \right). \tag{11}$$

Furthermore, (8) and (6) can be solved for R^2 and T^2, which yields the absolute values and phase angles of R and T as:

$$r = \sqrt{\left| \frac{S_4/S_2}{P_1^2} \right|}, \tag{12}$$

$$t = \sqrt{\left| \frac{S_2/S_1}{P_1^2} \right|}, \tag{13}$$

$$\varphi_R = \frac{1}{2} \angle \left(\frac{S_4/S_2}{P_1^2} \right), \tag{14}$$

$$\varphi_T = \frac{1}{2} \angle \left(\frac{S_2/S_1}{P_1^2} \right). \tag{15}$$

III. Results for Test Structures

In this section, we will first calculate the frequency-dependent wavenumber and attenuation parameter for our simulations. Then we will show, as an example, reflection, transmission, and scattering parameters for test structure TS1 ($h/\lambda = 2.5\%$). After this, we will summarize the parameter values for all studied structures and compare them to those of Lehtonen and Wang.

A. Wavenumber, SAW Velocity, and Attenuation

The procedure presented in Section II not only gives the wavenumber k as a function of frequency but it also allows for the determination of free-surface SAW velocity v. This is done by fitting a linear function to the frequency-dependent k data obtained using (11) and shown in Fig. 11, and comparing this line with:

$$k = \frac{\omega}{v} = \frac{2\pi f}{v}. \tag{16}$$

The fitting yields:

$$k = 0.00157910 \frac{1}{\mu\mathrm{m\,MHz}} f - 1.204323 \frac{1}{\mu\mathrm{m}}, \tag{17}$$

and comparison of the linear part of (17) with (16) gives:

$$v = \frac{2\pi f}{k} = \frac{2\pi}{0.00157910 \frac{1}{\mu\mathrm{m\,MHz}}} \approx 3978.97 \text{ m/s}. \tag{18}$$

The attenuation coefficient α can be transformed into propagation loss parameter $\gamma_{\lambda,\mathrm{dB}}$ giving the attenuation in decibels per wavelength

$$\gamma_{\lambda,\mathrm{dB}} = -20 \lg(e) \alpha\lambda \,\mathrm{dB} \approx -8.68 \alpha\lambda \,\mathrm{dB}. \tag{19}$$

The frequency-dependent $\gamma_{\lambda,\mathrm{dB}}$ obtained using (10) and (19) is shown in Fig. 12. The wavelength has been taken as $\lambda = v/f$. The mean propagation loss per wavelength (over 860 MHz to 1090 MHz) is about $-2.76 \cdot 10^{-4}$ dB. This value is very close to the expected $-2.73 \cdot 10^{-4}$ dB, the propagation loss parameter (independent of frequency) actually assumed in FEMSAW for these simulations (such a small attenuation parameter was used in order to exclude the propagation loss and hence to facilitate comparisons to earlier results). Some inaccuracy in the result is due to the definition of distances. Part of the distances L_i actually lie under metallization (half an electrode at each end).

B. Reflection, Transmission, and Scattering Parameters

Figs. 13 to 16 present the obtained r, t, φ_R, and φ_T for test structure TS1. The reflection coefficient has a magnitude r of a few percent, which increases with frequency. The magnitude t of the transmission coefficient is very close to 1 and decreases with frequency. The reflection phase φ_R is slightly less than $+90°$, and the transmission phase φ_T is a few degrees below zero, as expected.

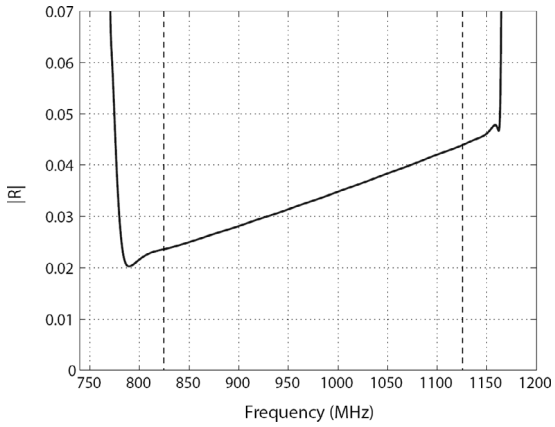

Fig. 13. Absolute value of R versus frequency for test structure TS1. Reliable region between dashed lines.

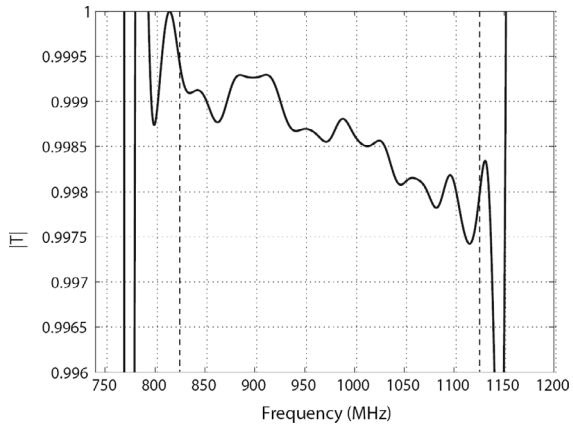

Fig. 14. Absolute value of T versus frequency for test structure TS1. Reliable region between dashed lines.

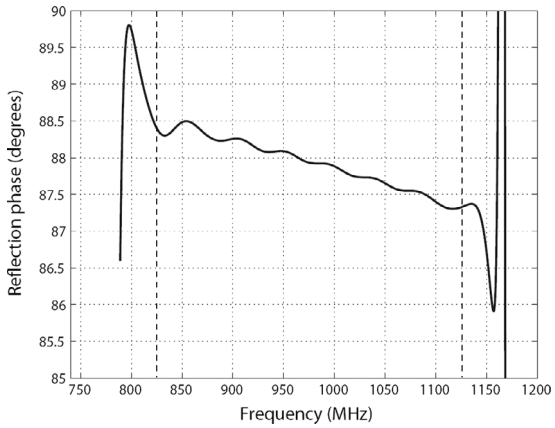

Fig. 15. Reflection phase φ_R versus frequency for test structure TS1. Reliable region between dashed lines.

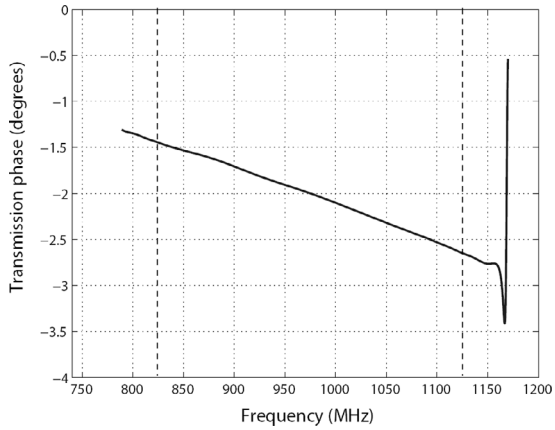

Fig. 16. Transmission phase φ_T versus frequency for test structure TS1. Reliable region between dashed lines.

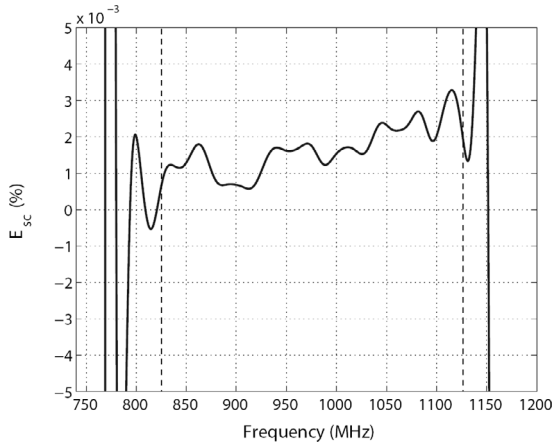

Fig. 17. Scattered energy E_{sc} versus frequency for test structure TS1. Reliable region between dashed lines.

Both phase shifts decrease with frequency. The conservation of energy is illustrated in Fig. 17, which presents the scattered energy defined as:

$$E_{\mathrm{sc}} = 1 - r^2 - t^2. \tag{20}$$

The reliable frequency range is roughly indicated by dashed lines in Figs. 11 to 17.

In order to compare the results obtained for all three test structures to those of Lehtonen and Wang, parameter values are averaged over the range from 950 MHz to 1050 MHz. When these mean values are compared to the results of Lehtonen and Wang (see Table III), a good agreement is observed, in general. The results for scattered energy in the case of $h/\lambda = 1.0\%$ are, however, visibly different but still of the same order. This is due to the fact that, for this metal thickness, the transmission coefficient is very close to 1 and accuracy is not sufficient.

IV. Conclusions

In this work, we have developed a method for determining the main reflection, transmission, and scattering

TABLE III
COMPARISON OF THE RESULTS FOR TEST STRUCTURES TS1, TS2, AND TS3 TO THOSE OF LEHTONEN (L) AND WANG (W).

	TS1	L	TS2	L	TS3	W
h/λ (%)	2.5		5.0		1.0	
a/p	0.4		0.6		0.5	
r	0.0348	0.034	0.0978	0.092	0.0305	0.0282
t	0.9985	—	0.9872	—	0.9993	0.9991
φ_R (°)	87.7	77.9	81.7	79.5	87.8	88.0
φ_T (°)	−2.3	−2.0	−6.8	−5.8	−2.0	−1.7
$E_{\rm sc}$ (%)	0.17	—	1.58	—	0.045	0.21
$E_{\rm sc}/r^2$	1.40	1.5	1.65	1.7	0.49	2.6

parameters for short metal reflectors. The method uses the FEM-BEM-computed S parameters of a SAW tag device to extract the reflection and transmission coefficients (absolute values and phase angles) and the energy scattered into bulk as a function of frequency. Assuming the S parameters available, this is a simple and very fast way to characterize single-electrode reflectors without heavy calculation or special software. Although only used for simulated data in this work, the same method can be applied to measured data as well.

ACKNOWLEDGMENTS

The authors are grateful to C. S. Hartmann, who proposed the idea of this method. S. Härmä thanks the Foundation of Technology (Finland) and the Nokia foundation for supporting her doctoral studies.

REFERENCES

[1] S. Härmä, V. Plessky, C. Hartmann, and W. Steichen, "Z-path SAW RFID tag," *IEEE Trans. Ultrason., Ferroelect., Freq. Contr.*, vol. 55, pp. 208–213, Jan. 2008.

[2] C. Hartmann, P. Brown, and J. Bellamy, "Design of global SAW RFID tag devices," in *Proc. 2nd Int. Symp. Acoust. Wave Devices for Future Mobile Commun. Syst.*, Mar. 2004, pp. 15–19.

[3] S. Lehtonen, V. Plessky, and M. Salomaa, "Short reflectors operating at the fundamental and second harmonics on 128° $LiNbO_3$," *IEEE Trans. Ultrason., Ferroelect., Freq. Contr.*, vol. 51, pp. 343–351, Mar. 2004.

[4] S. Lehtonen, V. Plessky, N. Bereux, and M. Salomaa, "Minimum-loss short reflectors on 128° $LiNbO_3$," *IEEE Trans. Ultrason., Ferroelect., Freq. Contr.*, vol. 51, pp. 1203–1205, Oct. 2004.

[5] S. Lehtonen, V. Plessky, N. Bereux, and M. Salomaa, "Phases of the SAW reflection and transmission coefficients for short reflectors on 128° $LiNbO_3$," *IEEE Trans. Ultrason., Ferroelect., Freq. Contr.*, vol. 51, pp. 1671–1682, Dec. 2004.

[6] W. Wang, T. Han, X. Zhang, H. Wu, and Y. Shui, "Rayleigh wave reflection and scattering calculation by source regeneration method," *IEEE Trans. Ultrason., Ferroelect., Freq. Contr.*, vol. 54, pp. 1445–1453, July 2007.

[7] T. Pastureaud, R. Lardat, W. Steichen, S. Ballandras, W. Daniau, and P. Berthelot, "Analysis of guided propagation using hybrid acoustic bulk and interdigital transducer," in *Proc. IEEE Ultrason. Symp.*, 2006, pp. 1866–1869.

[8] FEMSAW—An extremely accurate and powerful 2D FEM/BEM simulation tool for SAW devices, http://www.gvrtrade.com.

[9] P. Ventura, J. Hodé, M. Solal, J. Desbois, and J. Ribbe, "Numerical methods for SAW propagation characterization," in *Proc. IEEE Ultrason. Symp.*, 1998, pp. 175–186.

Sanna Härmä was born in Kotka, Finland, in 1977. She received the Master of Science and Licentiate of Science (in Technology) degrees from the Helsinki University of Technology (TKK), Espoo, Finland, in 2001 and 2007, and the Bachelor of Arts degree (in French philology) from the University of Helsinki, Helsinki, Finland, in 2007.

She has worked as a research assistant at the Laboratory of Biomedical Engineering, TKK, as a research scientist at the Materials Physics Laboratory, TKK, as a design engineer at Thales Microsonics, Sophia-Antipolis, France, and as a subject teacher in Helsinki, Finland. She is currently preparing a D.Sc. thesis on SAW RFID tags at the Laboratory of Optics and Molecular Materials, TKK.

Victor P. Plessky was born in Belarus in 1952. He received the Ph.D. degree from the Moscow Physical-Technical Institute in 1978 and the D.Sc. degree from the Institute of Radio Engineering and Electronics (IRE, Russian Academy of Sciences, Moscow) in 1987. He was awarded the USSR National Award for Young Scientists in 1984.

He started to work at IRE in 1978 as a junior researcher and was promoted to laboratory director in 1987. In 1991, he also worked as a part-time professor at the Patris Lumumba University, Moscow. He received the full professor title in 1995 from the Russian Government.

In 1992, he joined Ascom Microsystems SA, Bevaix, Switzerland, where he worked as a SAW project manager. Since 1997, he has lectured on various SAW topics at the Helsinki University of Technology (TKK), Espoo, Finland, as a visiting professor and currently holds a docentship at TKK. In 1998, he started to work at the Neuchâtel office (Switzerland) of Thomson Microsonics (later Thales Microsonics, finally Temex), and since 2002 he has worked as a consultant.

Dr. Plessky has been engaged in research on semiconductor physics, SAW physics (new types of waves, scattering and reflection on surface irregularities, and laser generation of SAW), SAW device development (filters, delay lines, and reflective array compressors), and magnetostatic wave studies. His current interests focus on SAW physics and low-loss SAW filter development.